



## **Constellations of Elliptical Inclined Lunar Orbits Providing Polar and Global Coverage**

**Todd A. Ely**

Jet Propulsion Laboratory  
California Institute of Technology  
4800 Oak Grove Drive  
Pasadena, California, 91109  
Email: [Todd.A.Ely@jpl.nasa.gov](mailto:Todd.A.Ely@jpl.nasa.gov)

**Erica Lieb**

ASRC Aerospace Corporation  
12021 Sunset Hills Rd. Suite 330  
Reston, VA 20190  
Email: [Erica.Lieb@akspace.com](mailto:Erica.Lieb@akspace.com)

# **AAS/AIAA Astrodynamics Specialists Conference**

**Lake Tahoe, CA, August 7-11, 2005**

**AAS Publications Office, P.O. Box 28130, San Diego, CA 92198**

(This page left intentionally blank)

# CONSTELLATIONS OF ELLIPTICAL INCLINED LUNAR ORBITS PROVIDING POLAR AND GLOBAL COVERAGE

Todd A. Ely<sup>1</sup> and Erica Lieb<sup>2</sup>

Prior results have developed a methodology for selecting a long-lived constellation of 3 satellites that provide persistent, stable coverage to either the North or South Pole with no requirement for stationkeeping under the influence of only gravitational perturbations. In the present study, the sensitivity of this coverage in the presence of non-gravitational forces is determined, and a design strategy is formulated that minimizes any potential sensitivity to these accelerations. The class of orbits and methods are extended to the search for global coverage constellations of 6 satellites. Two constellations are designed that provide 99.9999% global coverage for a 10 year period also without the need for any deterministic orbit maintenance.

## INTRODUCTION

With the announcement of the President's exploration vision in January 2004 and the Moon as a destination for human exploration, the need to investigate desirable orbits for designing constellations of satellites providing in-situ lunar communication and navigation services has risen. In a prior study by Ely [1] a methodology was developed for selecting a constellation of 2 or 3 satellites to provide persistent, stable coverage to either the North or South Pole with no requirement for stationkeeping under the influence of gravitational perturbations. In the current study, the impact on the aforementioned coverage properties from non-conservative perturbations (i.e., solar radiation pressure) is investigated. Preliminary results indicate that accommodations for solar radiation pressure can be made by making adjustments to the semi-major axis with the result that the 2-fold coverage remains persistent at the poles. This initial result suggests that control requirements can still be minimized by appropriate orbit selection.

The class of orbits utilized for designing the Polar coverage constellation can also be used to design global coverage constellations. Indeed, constellations of elliptical inclined orbits that circulate in  $e - \omega^{op}$  phase plane are found to provide global coverage 99.9999% of the time using only 6 satellites. The orbital elements for two global coverage constellations are found with the same methodology that was used to select orbits for the Polar coverage constellation. The configuration for the constellations

---

<sup>1</sup> Senior Engineer, Guidance, Navigation, and Control Section, Jet Propulsion Laboratory, California Institute of Technology, MS 301-125L, 4800 Oak Grove Drive, Pasadena, CA 91109-8099. Ph: 818-393-1744, Email: [Todd.A.Ely@jpl.nasa.gov](mailto:Todd.A.Ely@jpl.nasa.gov).

<sup>2</sup> Aerospace Engineer, Office of Spectrum Management, ASRC Aerospace, 12021 Sunset Hills Rd. Suite 330, Reston, VA 20190. Ph: 571-262-3134. Email: [Erica.Lieb@akspace.com](mailto:Erica.Lieb@akspace.com).

employs two orbital planes of 3 elliptical inclined orbits in each plane. The planes are separated by  $90^\circ$  and apoapsis is oriented oppositely between planes. Notionally these orbits form a *linked chain*. These constellations also maintain persistent coverage without the need for any explicit deterministic control during a nominal operational lifetime of 10 years.

## LIBRATING AND CIRCULATING ELLIPTICAL INCLINED LUNAR ORBITS

For the class of orbits being considered in this study the Earth produces the most significant perturbations. Perturbations from other sources such as the Sun, the Moon's non-spherical gravity field, and, depending on the specific satellite configuration, solar radiation pressure are secondary effects. In Ref. [1] simplified equations for the mean motion of the satellite orbits that are amenable to a qualitative analysis are derived and take the form,

$$\frac{de}{dt} = \frac{15}{8} \gamma \frac{n_E^2}{n} e \sqrt{1-e^2} \sin^2 i^{\text{op}} \sin 2\omega^{\text{op}}, \quad (1)$$

$$\frac{d\omega^{\text{op}}}{dt} = \frac{3}{8\sqrt{1-e^2}} \gamma \frac{n_E^2}{n} [(5 \cos^2 i^{\text{op}} - 1 + e^2) + 5(1 - e^2 - \cos^2 i^{\text{op}}) \cos 2\omega^{\text{op}}]. \quad (2)$$

Where orbital elements with a superscript 'op' are reconciled in a frame at the Moon with z-axis parallel to the normal of the Earth's apparent orbit around the Moon, the mass ratio is defined as  $\gamma = \frac{m_E}{m_E + m_M}$  with  $m_M$  the mass of the Moon,  $m_E$  the mass of the Earth,

the mean motion of the Earth around the Moon is  $n_E = \sqrt{\frac{G(m_E + m_M)}{a_E^2}}$  and the mean

motion of the spacecraft is  $n \equiv \sqrt{\frac{Gm_M}{a^3}}$ . It should be noted that in the above model that

the semi-major axis  $a$  is a constant of motion, and the inclination  $i$  and ascending node  $\Omega$  are completely determined by solutions for  $e - \omega^{\text{op}}$ , that is,  $i(e, \omega^{\text{op}})$  and  $\Omega(i, \omega^{\text{op}})$ .

Solutions to Eqs. (1) and (2) of particular interest are the stable librations of  $e - \omega^{\text{op}}$  around the fixed point solutions where  $e - \omega^{\text{op}}$  remain constant (i.e.,  $\frac{de}{dt} = \frac{d\omega^{\text{op}}}{dt} = 0$ ).

Examination of the equations reveals the fixed point solutions when the following conditions are met,

$$\sin 2\omega^{\text{op}} = 0, \quad (3)$$

and,

$$(5 \cos^2 i^{\text{op}} - 1 + e^2) + 5(1 - e^2 - \cos^2 i^{\text{op}}) \cos 2\omega^{\text{op}} = 0, \quad (4)$$

which leads to the following results,

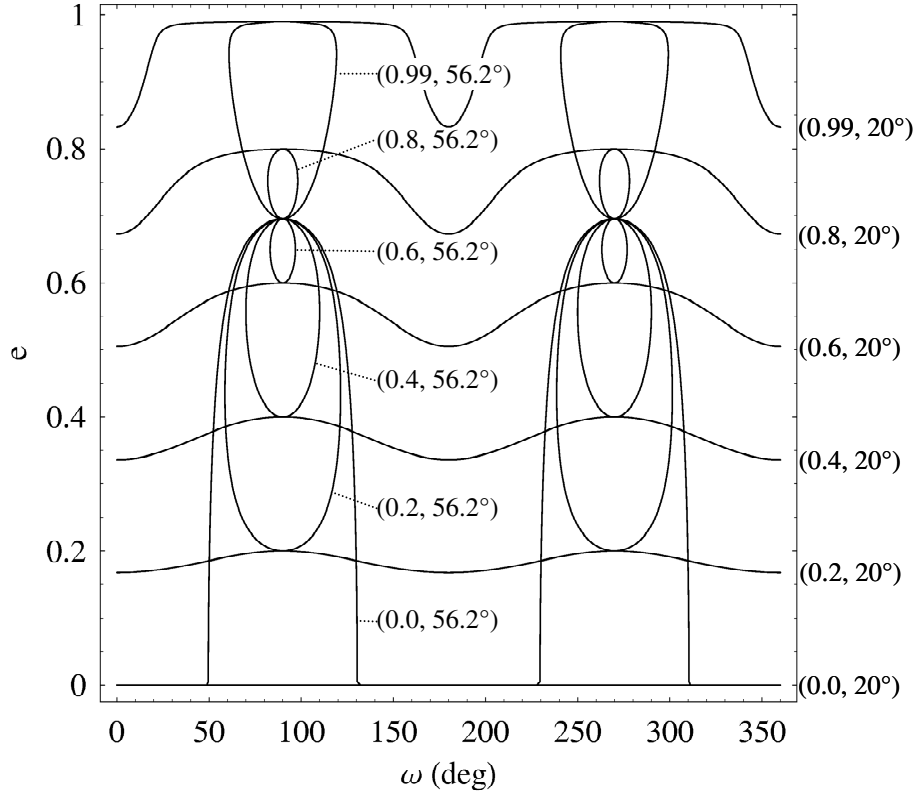


**Figure 1:** Trajectories in the  $e - \omega^{\text{op}}$  phase plane for selected initial values of eccentricity and inclination  $(e_0, i_0^{\text{op}})$ . All trajectories have initial argument's of periapsis  $\omega^{\text{op}} = 90^\circ$  or  $270^\circ$ . In general, trajectories with initial inclinations above  $39.6^\circ$  will librate, and below this value will circulate.

$$\omega^{\text{op}} = 90^\circ, 270^\circ \text{ and } e^2 + \frac{5}{3} \cos^2 i^{\text{op}} = 1. \quad (5)$$

In addition to the particular fixed point solutions, Eqs. (1) and (2) are completely integrable with the following general solution,

$$(1 - e^2) \cos^2 i^{\text{op}} \equiv \alpha \quad (6)$$

and,

$$e^2 \left( 1 - \frac{5}{2} \sin^2 i^{\text{op}} \sin^2 \omega^{\text{op}} \right) \equiv \beta = \frac{5}{2} R + \frac{15}{8} \alpha. \quad (7)$$

where  $\alpha$  is a constant of motion and is related to the z-component of the angular momentum and  $\beta$  is a constant of motion related to the disturbing function (also a constant of motion) and  $\alpha$  (c.f., the last term in Eq. (7)). Figure 1 illustrates some example trajectories resulting from solutions to Eqs. (6) and (7) in the  $e - \omega^{\text{op}}$  phase plane. Note that two types of trajectories for  $e - \omega^{\text{op}}$  motion are illustrated: closed librations and open circulations. The paired sets of numbers shown on the figure are the

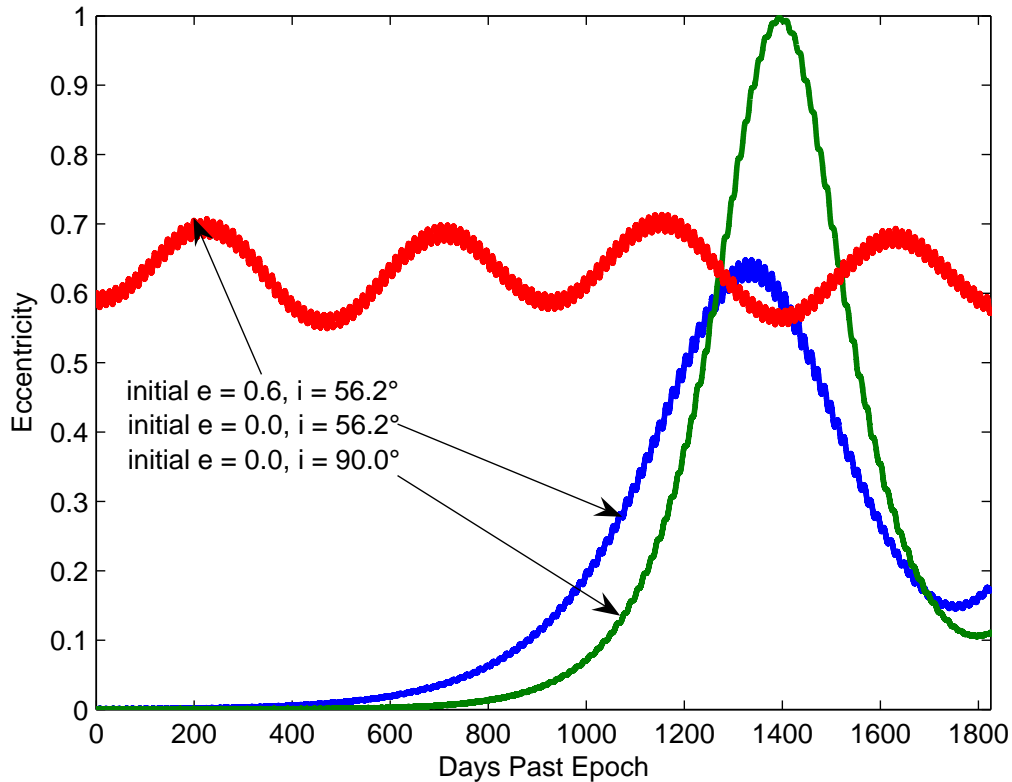


**Figure 2:** 5 year propagations of an elliptical inclined orbit, a circular inclined orbit, and a circular polar orbit.

initial eccentricity and inclination for each trajectory; all trajectories begin with an initial argument of periapsis value that is either  $90^\circ$  or  $270^\circ$ . The division between open or closed motions occurs when  $\beta = 0$  which exists either for  $e = 0$  or for  $i^{\text{op}} = \sin^{-1}(\sqrt{2/5}) \approx 39.2^\circ$  (often called the ‘critical inclination’ in the 3<sup>rd</sup> body perturbed problem).

An attractive feature of either the circulating or librating eccentric inclined orbits is their characteristic quasiperiodic behavior that produces an inherent bounded stability. This is not necessarily true for the case of circular orbits. Indeed previous research has revealed lunar orbits perturbed by the Earth show an array of dynamic behaviors that indicate the possibility of a circular orbit transitioning to a hyperbolic trajectory or even chaotic [2]. An example of this comparison is illustrated in Figure 2 showing 5-year propagations beginning 15-Jul-2009 1 PM ET of three orbits that include inverse square gravity and the Earth as the only perturbing acceleration. The initial conditions for each orbit have as common data  $\{a, \Omega^{\text{op}}, \omega^{\text{op}}, M\} = \{6542 \text{ km}, 0^\circ, 90^\circ, 0^\circ\}$  and the eccentricity and the inclination differ for each orbit. The elliptical orbit with  $(e_o, i_o^{\text{op}}) = (0.6, 56.2^\circ)$  represents a librating solution of Eqs. (6) and (7) corresponding to  $\alpha = 0.198414$  and  $\beta = -0.26098$ . This solution yields a variation of eccentricity  $e \in (0.6, 0.7)$  which is

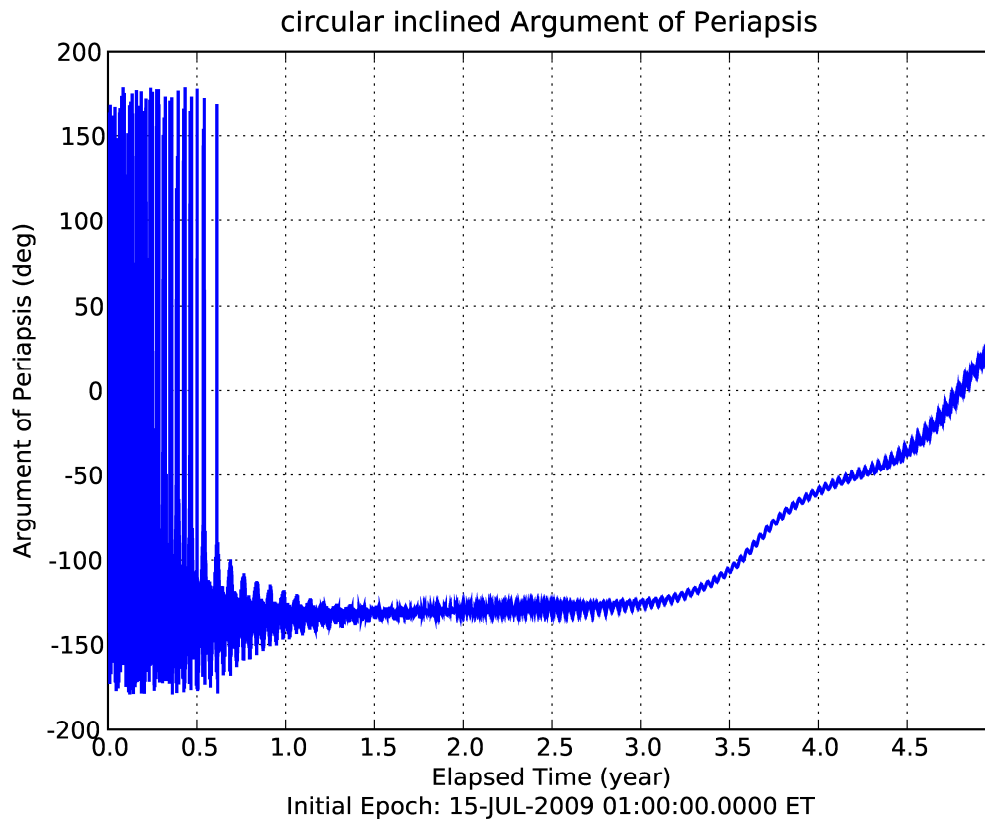


**Figure 3:** 5 year argument of periapsis history for the circular orbit with initial inclination of  $56.2^\circ$

corroborated by the numerical results in Figure 2. This particular orbit is important because it will be used in the next section as the basis for designing a constellation providing continuous South Pole coverage. The second orbit has the same initial inclination as the elliptical orbit. It represents a degenerate solution to Eqs. (6) and (7) yielding the separatrix between librating and circulating motion. The numerically propagated solution for the argument of periapsis shown in Figure 3 reveals that this orbit is initially circulating, and then after about a  $\frac{3}{4}$  of a year it transitions into libration. The eccentricity history then follows the curve leading to a maximum around 0.6. Note that the maximum eccentricity is not 0.7 as with the initially elliptic orbit because this orbit starts with a different  $\alpha$  and  $\beta$  because of an initial zero eccentricity. Finally, the third orbit is a circular polar orbit, and illustrates the possibility of a circular orbit becoming nearly hyperbolic in a finite time. These three orbits illustrate the fundamental bounded stability offered by orbits with initial conditions starting near the frozen conditions prescribed by Eq. (5).

## POLAR COVERAGE CONSTELLATION

A great deal of scientific interest exists regarding the permanently shadowed craters near the poles of the Moon where there may be frozen volatiles. These regions, particularly

the Moon's South Pole, have been proposed for extensive robotic and human exploration. Ely [1] proposed a constellation of 3 orbiters in a common plane that utilizes the librating orbit solutions presented in the previous section to provide continuous 2-fold coverage to either the South or North Pole that is persistent and stable as the orbits evolve naturally under the influence of gravitational accelerations. In that study, the constellation was designed such that the relative mean anomaly spacing between the orbiters exhibited near zero secular drift. This fundamental characteristic leads to stable coverage characteristics in spite of the fact that the orbits have pronounced eccentricity variations of  $\Delta e \sim 0.1$  and inclination variations of  $\Delta i^{\text{op}} \sim 5^\circ \rightarrow \Delta i^{\text{ep}} \sim 15^\circ$  (where the 'ep' refers to the inclination variation resolved in the Moon's IAU equatorial frame). The specific solution for a 3-satellite constellation yields the following initial elements,

$$\begin{aligned} \{a_1, e_1, i_1^{\text{op}}, \Omega_1^{\text{op}}, \omega_1^{\text{op}}, M_1\} &= \{6541.4 \text{ km}, 0.6, 56.2^\circ, 0^\circ, 90^\circ, 0^\circ\}, \\ \{a_2, e_2, i_2^{\text{op}}, \Omega_2^{\text{op}}, \omega_2^{\text{op}}, M_2\} &= \{6543.9508164 \text{ km}, 0.6, 56.2^\circ, 0^\circ, 90^\circ, 120^\circ\}, \\ \{a_3, e_3, i_3^{\text{op}}, \Omega_3^{\text{op}}, \omega_3^{\text{op}}, M_3\} &= \{6537.8985219 \text{ km}, 0.6, 56.2^\circ, 0^\circ, 90^\circ, 240^\circ\} \end{aligned} \quad (8)$$

at an epoch of 15-Jul-2009 1 PM ET. The methodology used to select the initial semi-major axis values is propagate all three orbits for a period of time (2 years in this study), and solve for a delta semi-major axis that would arrest any secular relative mean anomaly drift between the satellites. This process is iterated until a selected convergence is achieved. Detailed numerical analysis [1] of the long term evolution of these orbits has shown that the coverage at South Pole is continuous and 2-fold for a period of at least 10 years.

The constellation defined in Eq. (8) was found using only gravitational accelerations from the Moon (spherical and non-spherical), the Earth, and the Sun. In the present work the accelerations have been expanded to include non-gravitational accelerations from solar radiation pressure. The goal is to determine to what extent the original methodology developed in Ref. [1] is still applicable for designing the constellation such that it maintains the original property of continuous 2-fold coverage at the South Pole. The characteristics of the simulated spacecraft and solar radiation parameters are identified in Table 1. Note that the solar radiation pressure model accounts for shadowing of the Sun by the Moon and computes entry/exit through the umbra and penumbra of these shadows.

**Table 1:** Identification of Spacecraft and Solar Radiation Parameter Values

Parameter	Value
Spacecraft Mass	1075 kg
Spacecraft Shape	Sphere of radius 3.47 m $\rightarrow$ 37.9 m <sup>2</sup> surface area
Diffuse Reflectivity Coefficient	0.3
Solar Flux at 1 A.U.	0.1020506244e+09 kg-km <sup>3</sup> /m <sup>2</sup> -sec <sup>2</sup>

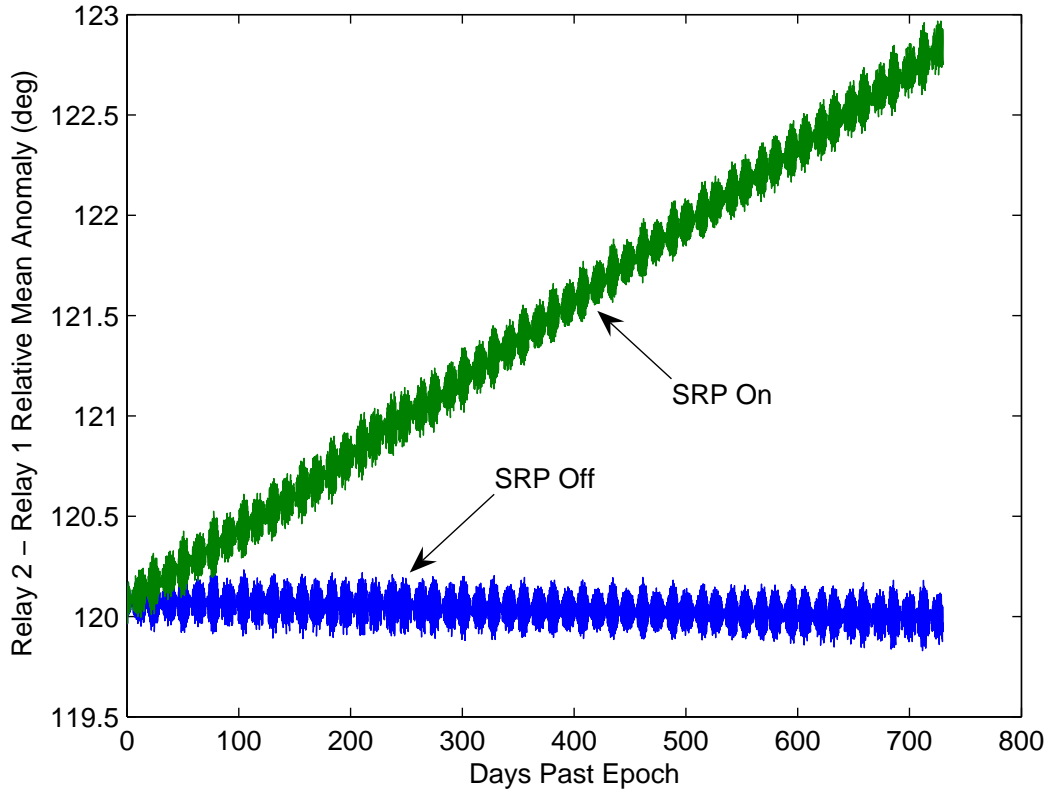


**Figure 4:** Comparison of relative mean anomaly of between first two satellites in the 3 satellite Polar constellation designed to maintain a near constant spacing with solar pressure turned off (horizontal line) as compared to the same orbits with solar pressure turned on (sloped line).

Propagating with this model, it is found that the solar radiation pressure induces a predominantly secular change. This is seen in Figure 4, which compares the relative mean anomaly spacing between the first and second satellite orbits that were designed in the presence of only gravity perturbations (indicated by ‘SRP off’), and the same orbits with solar pressure turned on (indicated by ‘SRP on’). It is evident that the relative mean anomaly exhibits little or no secular shift when solar pressure is off (the design case). With solar pressure on, the relative mean anomalies exhibit a secular drift of about 0.3 deg/year. The fix for eliminating this drift is the same as before; adjust the semi-major axis values to arrest the secular drift. Doing so yields the following estimates for the elements,

$$\begin{aligned}
 \{a_1, e_1, i_1^{\text{op}}, \Omega_1^{\text{op}}, \omega_1^{\text{op}}, M_1\} &= \{6541.4 \text{ km}, 0.6, 56.2^\circ, 0^\circ, 90^\circ, 0^\circ\}, \\
 \{a_2, e_2, i_2^{\text{op}}, \Omega_2^{\text{op}}, \omega_2^{\text{op}}, M_2\} &= \{6543.9758657 \text{ km}, 0.6, 56.2^\circ, 0^\circ, 90^\circ, 120^\circ\}. \quad (9) \\
 \{a_3, e_3, i_3^{\text{op}}, \Omega_3^{\text{op}}, \omega_3^{\text{op}}, M_3\} &= \{6537.9213419 \text{ km}, 0.6, 56.2^\circ, 0^\circ, 90^\circ, 240^\circ\}
 \end{aligned}$$

The addition of solar pressure induced only small changes in semi-major axis for the 2<sup>nd</sup> and 3<sup>rd</sup> spacecraft of  $\Delta a_2 = 0.0250493$  km and  $\Delta a_3 = 0.0228199$  km, respectively.

It should be emphasized that this constellation maintains its relative configuration and continuous coverage of the South Pole without the need for any deterministic control. It is certainly expected that the satellites would require some form of active orbit control to account for errors and other non-gravitational effects (i.e., spacecraft outgassing, uncoupled momentum desaturations, etc.), however none is needed to correct for effects due to gravity or the ‘gross’ effects of solar radiation pressure. However, it should be noted that solar radiation pressure effects due to a non-spherical spacecraft shape that may be pointing has not been examined for its impact on orbit evolution.

## GLOBAL COVERAGE *LINKED-CHAIN* CONSTELLATIONS

In addition to focused coverage at the poles, NASA’s interests include global coverage as well. The circulating orbit solution, rather than the librating solution used for the Polar coverage constellation, can be used to design constellations with bounded stability in eccentricity and persistent global coverage for at least a 10 year period. The central notion for these constellations is the observation that the single plane in the Polar constellation yields an ‘eccentric street of coverage’ on the surface of an underlying non-rotating celestial sphere. This is a coverage pattern that produces a swath on the surface of the celestial sphere that begins and terminates along the celestial track of the orbital plane. The idea now is to add an orbit plane that is rotated by  $90^\circ$  in ascending node with orbits that have their apoapsis  $180^\circ$  opposite of those in the original plane. In this configuration, the second eccentric street from the additional orbit plane fills the coverage gaps left by the original plane, that is, the streets form a *linked-chain*. For this configuration, it is desirable to exploit the circulating orbit concept for all of the orbits such that the entire configuration maintains global coverage without the need for an explicit control strategy. Two constellations have been designed consisting of only 6 satellites that each provide 99.9999% global coverage for a 10 year period.

Ideally an efficient global coverage constellation distributes its coverage evenly over the surface of the planet. This is indeed the motivation behind the constellations designed by John Walker [3] where he discovered a 5 satellite inclined circular orbit configuration that provides global coverage, which is to date, the smallest number of satellites in circular orbits that provide global coverage. In the present study, efficiency using orbits with near circular orbits to provide global coverage motivated a search for a class of slightly elliptical orbits exhibiting a  $e - \omega^{\text{op}}$  circulation with an associated small variation in eccentricity. Additionally, these orbits should possess sufficient inclination to minimize biases in coverage between the poles and the equator. Recall, that the division between circulation and libration occurs at the ‘critical value’ of  $39.2^\circ$ . An illustration of the circulating solutions at  $39^\circ$  and the librating solutions at  $40^\circ$  are shown in Figure 5. The relevant observation is that for circulating orbits with an initial argument of periapsis at either  $\omega^{\text{op}} = 90^\circ$  or  $270^\circ$  the eccentricity is at its maximum value. As an illustration, the curve associated with the initial condition  $(e, i^{\text{op}}, \omega^{\text{op}}) = (0.1, 39^\circ, 90^\circ)$  is

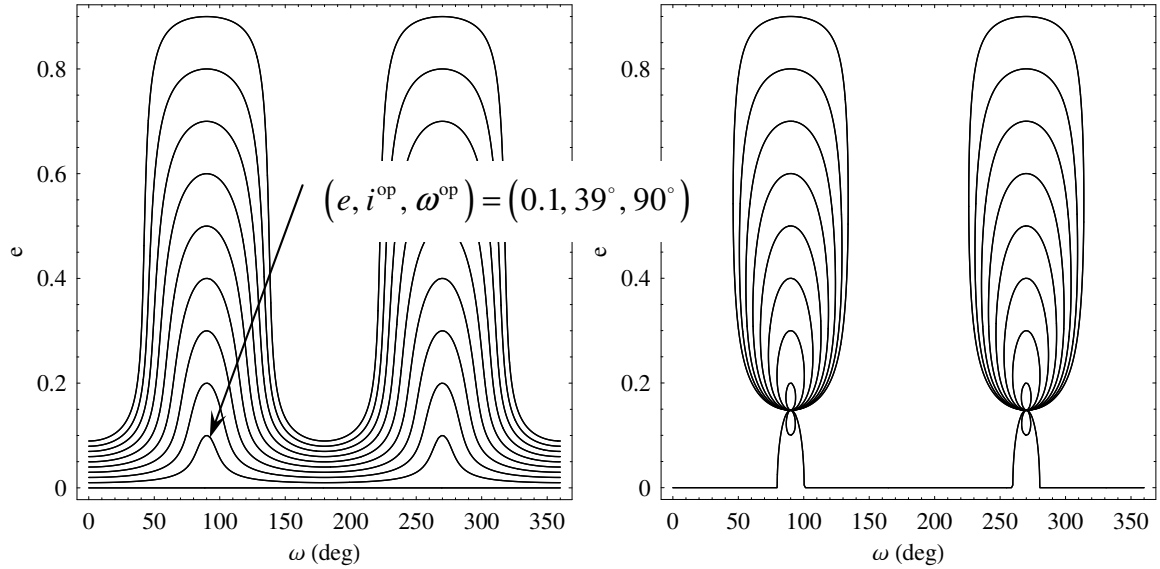


**Figure 5:** Trajectories in the  $e - \omega^{\text{op}}$  phase plane for selected initial values of eccentricity between (0.0, 0.9) in 0.1 increments and inclination of  $39^\circ$  on the left, and an inclination of  $40^\circ$  on the right. All trajectories have initial argument's of periapsis  $\omega^{\text{op}} = 90^\circ$  or  $270^\circ$ . The trajectories on the left circulate and those on the right librate.

identified by the callout in Figure 5. This suggests a strategy for selecting desirable circulating orbits is to choose initial conditions at these points with the anticipation that subsequent values of eccentricity will be less than the initial condition.

Now, consider that higher order effects and other accelerations beside Earth gravity destroy the exact solutions given by Eqs. (6) and (7) solutions. A series of numerical investigations were conducted to better understand these effects. It was found that libration solutions at inclinations in a region near the critical value did not always exist for eccentricities above zero (which is predicted by the approximate theory). In fact, there

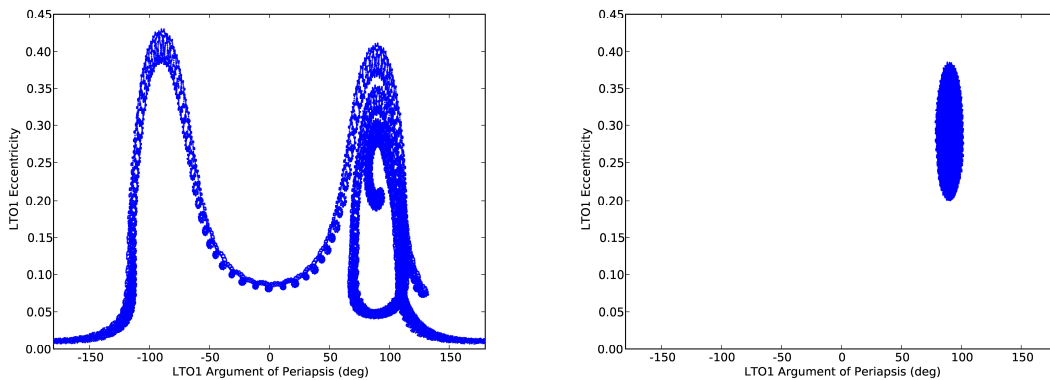


**Figure 6:**  $e - \omega^{\text{op}}$  phase plane of an orbit exhibiting both circulation and libration on the left for an initial eccentricity of 0.2, and just libration on the right with an initial eccentricity of 0.3.

were examples of trajectories that transitioned between circulation and libration within the defining ten year period that this study is concerned with. Example  $e - \omega^{\text{op}}$  phase plots for ten year propagations are shown in Figure 6 with  $(a, e, i^{\text{op}}, \omega^{\text{op}}) = (9873 \text{ km}, 0.2, 45^\circ, 90^\circ)$  on the left, and  $(a, e, i^{\text{op}}, \omega^{\text{op}}) = (9873 \text{ km}, 0.3, 45^\circ, 90^\circ)$  on the right. The left trajectory begins in a near libration centered on  $\omega^{\text{op}} = 90^\circ$  and then transitions into circulation, while the right trajectory remains in a libration. The analytic solution would predict libration for both cases. This example illustrates the complexities of the real system with potential for chaotic transitions to occur. Numerical investigations also indicated that for lower eccentricities and inclinations the propensity to exhibit this transition decreases. A detailed study of the phase space using mean element propagations is required to better understand the characteristics of these motions. This is a subject of a follow-on investigation.

### Global Coverage Constellation A

With the preceding observations in mind a 6 satellite constellation with an initial inclination of  $40^\circ$  (sufficient to cover the poles) and eccentricity of 0.05 providing global coverage was sought. Starting with an initial 9500 km semi-major axis and propagating for 50 days, global coverage of sample constellations were examined. This process was repeated with smaller values of semi-major axis until coverage gaps were discovered. It was found that at 7000 km the constellation stopped providing global coverage over the 50 day span. A thorough study at the 7500 km semi-major axis was then conducted with the same techniques used in the Polar coverage constellation to tune semi-major axis values that provide stable relative mean anomaly spacing. For this proposed constellation the final results for the constellations first plane are,

$$\begin{aligned} \{a_1, e_1, i_1^{\text{op}}, \Omega_1^{\text{op}}, \omega_1^{\text{op}}, M_1\} &= \{7500.0 \text{ km}, 0.05, 40^\circ, 0^\circ, 90^\circ, 0^\circ\}, \\ \{a_2, e_2, i_2^{\text{op}}, \Omega_2^{\text{op}}, \omega_2^{\text{op}}, M_2\} &= \{7509.3440409 \text{ km}, 0.05, 40^\circ, 0^\circ, 90^\circ, 120^\circ\}, \\ \{a_3, e_3, i_3^{\text{op}}, \Omega_3^{\text{op}}, \omega_3^{\text{op}}, M_3\} &= \{7499.2237825 \text{ km}, 0.05, 40^\circ, 0^\circ, 90^\circ, 240^\circ\} \end{aligned} \quad (10)$$

and results for the second plane are,

$$\begin{aligned} \{a_4, e_4, i_4^{\text{op}}, \Omega_4^{\text{op}}, \omega_4^{\text{op}}, M_4\} &= \{7500.0 \text{ km}, 0.05, 40^\circ, 90^\circ, 270^\circ, 0^\circ\}, \\ \{a_5, e_5, i_5^{\text{op}}, \Omega_5^{\text{op}}, \omega_5^{\text{op}}, M_5\} &= \{7494.6802266 \text{ km}, 0.05, 40^\circ, 90^\circ, 270^\circ, 120^\circ\}, \\ \{a_6, e_6, i_6^{\text{op}}, \Omega_6^{\text{op}}, \omega_6^{\text{op}}, M_6\} &= \{7504.8294193 \text{ km}, 0.05, 40^\circ, 90^\circ, 270^\circ, 240^\circ\} \end{aligned} \quad (11)$$

beginning with an epoch of July 1, 2015 1 AM ET. As with the Polar coverage constellation, no explicit control is required to correct for the natural motions under the influence of gravitational accelerations and solar radiation pressure accelerations. The configuration of this constellation is illustrated in Figure 7. The graphic on the left illustrates the first plane of the constellation and a snapshot of the coverage that it provides on the surface (note the coverage gap indicated by the callout). The graphic on the right illustrates the entire constellation looking edge-on of the second plane. The addition of the second plane eliminated the coverage gap seen to the left. The long term

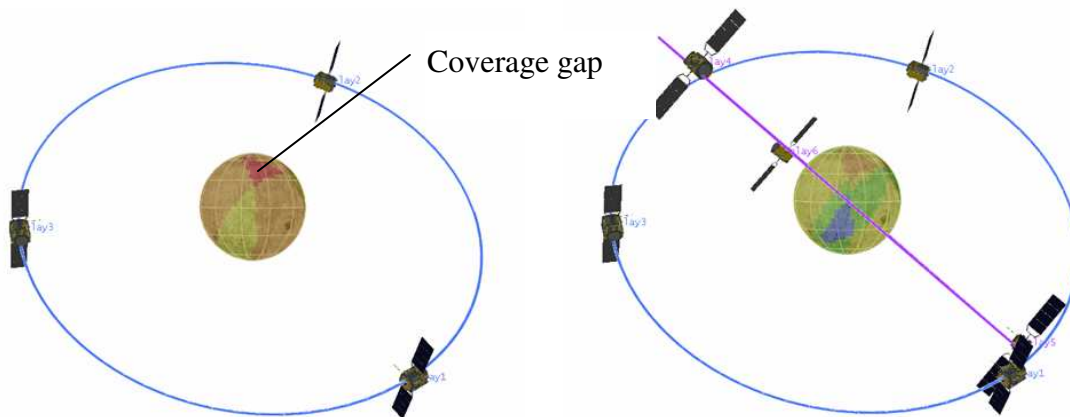


**Figure 7:** Configuration of the first 6 satellite global coverage constellation with semi-major axis of 7500 km. The graphic on the left illustrates the first plane of the constellation, and the graphic on the right illustrates the entire constellation looking edge-on of the second plane.

behavior of the  $e - \omega^{\text{op}}$  phase plane for this constellation was assessed for a 10 year propagation, and a 100 year propagation with the results shown in Figure 8 for the constellation's 6<sup>th</sup> satellite. Both figures illustrate a predominantly circulating result. For 10 years the eccentricity growth remains below 0.1, however in later years as argument of periapsis completes a full circuit the maximum eccentricity begins to grow. However, for the entire 100 years the periapsis altitude is regularly above 3500 km indicating the presence of a bounded stability. The central question is, of course, "Does this constellation provide persistent global coverage for the initial 10 year period?" This is addressed next.

Because the orbits under investigation do not conform to any standard analytic theory there are no simple tools to compute coverage characteristics for the duration of the trajectories. Numerical simulations collecting coverage statistics to a distribution of lunar surface assets as the orbits evolve had to be used. The statistics were computed using two tools; the first, is a tool built around JPL's institutional operational navigation software, and the other is STK<sup>TM</sup>. Each tool's results were used to validate those computed by the other. The JPL tool used a grid of stations separated by  $10^\circ$  in longitude and  $5^\circ$  in latitude that were poled every 4 hours to determine the number of spacecraft in-view. The STK<sup>TM</sup> simulations used a grid of surface assets separated by  $10^\circ$  in both longitude and latitude, and conducted an event search to find rise/set times to the millisecond accuracy. STK<sup>TM</sup> took longer to run but returned more detailed specifics on the nature of the outages for the two year propagations. The JPL tool was used primarily to collect aggregate statistics over the 10 year propagations. The average folds of coverage as a percentage of the Moon's surface area have been computed for 10 years with the results tabulated Table 2.

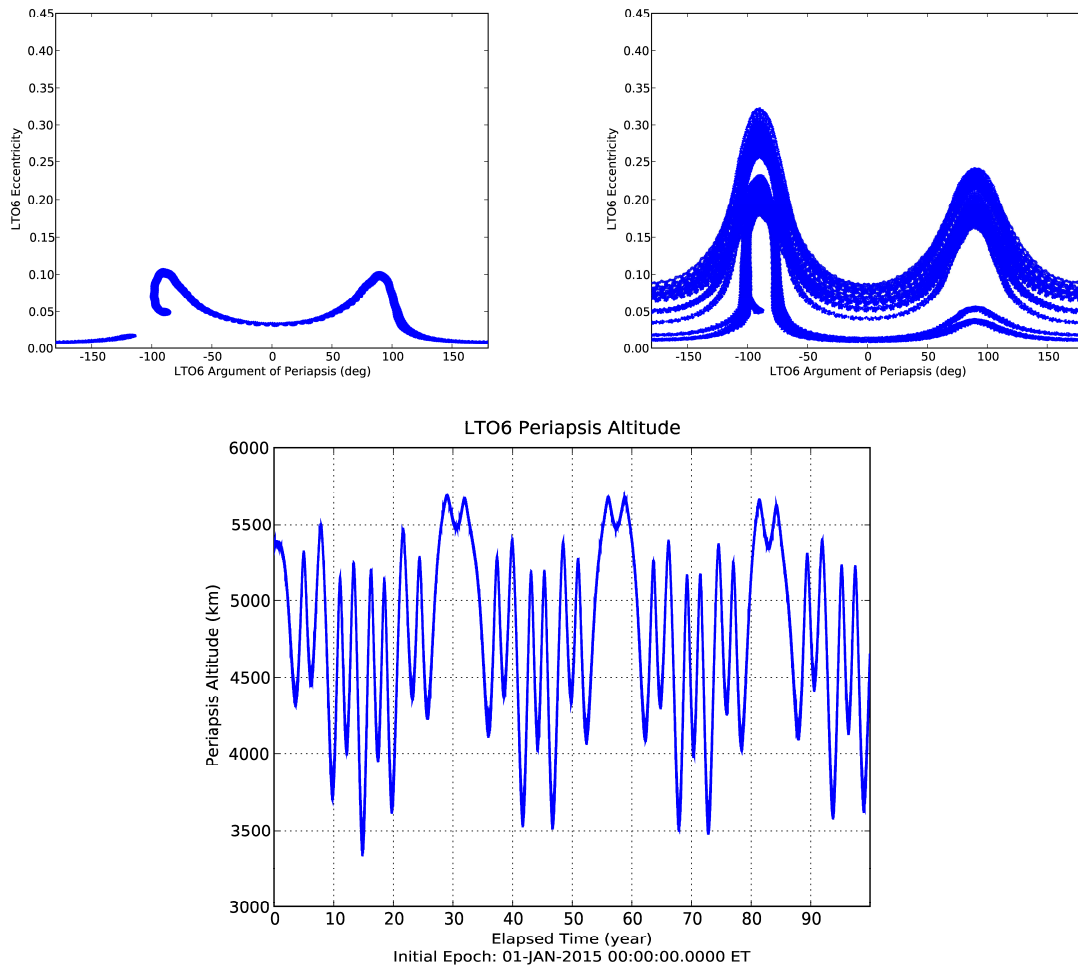


**Figure 8:** Global Constellation A’s 6<sup>th</sup> satellite  $e - \omega^{op}$  phase plane for 10 years (upper left) and 100 (upper right), and periapsis altitude for the 100 years (lower).

**Table 2: Average Folds of Coverage over 10 Years for Global Constellation A**

Fold of Coverage	Average % Surface Area Covered
0-fold (no coverage)	0.00005
1-fold or more	99.99995
2-folds or more	92.7
3-folds or more	33.9
4-folds	3.8

The 2-year coverage results found using STK™ show that the constellation has some outages, however their occurrence is brief and few. The maximum duration is 7.4 minutes and the total duration for the 2 years is 96 min (out of a total of 525600 min). The detailed plot of these outages is illustrated in Figure 9. For all practical purposes this constellation provides global coverage with minimal outages. Indeed, most of the time the constellation provides 2 satellites in view. This is an important feature if the

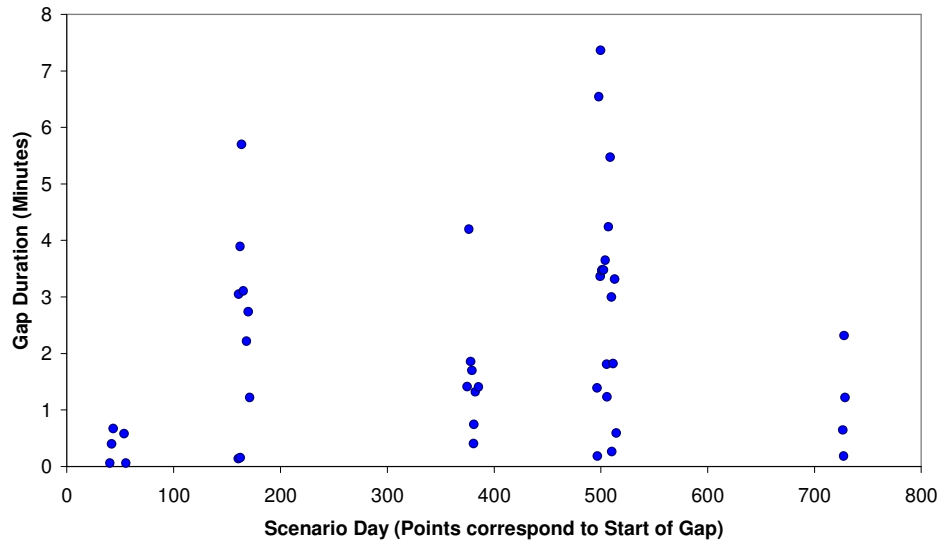


**Figure 9:** Constellation A's coverage outage history in its first two years.

constellation is to provide navigation services, because two satellites in-view is sufficient for a surface user to solve for their latitude and longitude instantaneously using 2-Way range to the satellites. Furthermore, the extended 10 year results show that the coverage is persistent without the need for *any* scheduled orbit maintenance.

### Global Coverage Constellation B

This second constellation has been designed using the same methodology and fundamental configuration characteristics as was used for the first; the primary differences are the target eccentricity increased from 0.05 to 0.185, and the target semi-major axis increased from 7500 km to 9873 km. As will be seen, a key qualitative characteristic of the long term propagation for Constellation B that differs from Constellation A is that the 100 year history for the eccentricity remains below 0.2, whereas for the former the eccentricity neared 0.35 during the same period. Because this constellation has a larger semi-major axis and eccentricity it is not as efficient as the first, however it does exhibit a circulation in  $e - \omega^{\text{op}}$  that is more consistent over the 100 years. This suggests that coverage properties in the second decade of the constellation may be better behaved than with the first, this is an open question that will be investigated in later studies.

The orbit solutions for the first plane of this second constellation are given by,

$$\begin{aligned}
 \{a_1, e_1, i_1^{\text{op}}, \Omega_1^{\text{op}}, \omega_1^{\text{op}}, M_1\} &= \{7500.0 \text{ km}, 0.05, 40^\circ, 0^\circ, 90^\circ, 0^\circ\}, \\
 \{a_2, e_2, i_2^{\text{op}}, \Omega_2^{\text{op}}, \omega_2^{\text{op}}, M_2\} &= \{7509.3440409 \text{ km}, 0.05, 40^\circ, 0^\circ, 90^\circ, 120^\circ\} \quad (12) \\
 \{a_3, e_3, i_3^{\text{op}}, \Omega_3^{\text{op}}, \omega_3^{\text{op}}, M_3\} &= \{7499.2237825 \text{ km}, 0.05, 40^\circ, 0^\circ, 90^\circ, 240^\circ\}
 \end{aligned}$$

and results for the second plane are,

$$\begin{aligned} \{a_4, e_4, i_4^{\text{OP}}, \Omega_4^{\text{OP}}, \omega_4^{\text{OP}}, M_4\} &= \{7500.0 \text{ km}, 0.05, 40^\circ, 90^\circ, 270^\circ, 0^\circ\}, \\ \{a_5, e_5, i_5^{\text{OP}}, \Omega_5^{\text{OP}}, \omega_5^{\text{OP}}, M_5\} &= \{7494.6802266 \text{ km}, 0.05, 40^\circ, 90^\circ, 270^\circ, 120^\circ\}, \\ \{a_6, e_6, i_6^{\text{OP}}, \Omega_6^{\text{OP}}, \omega_6^{\text{OP}}, M_6\} &= \{7504.8294193 \text{ km}, 0.05, 40^\circ, 90^\circ, 270^\circ, 240^\circ\} \end{aligned} \quad (13)$$

with an initial epoch of July 1, 2015 1 AM ET. The constellation’s 10 year and 100 year  $e - \omega^{\text{OP}}$  phase plots and 100 year periapsis altitude history for the 6<sup>th</sup> satellite are shown in Figure 10. As compared to Constellation A’s  $e - \omega^{\text{OP}}$  phase plane results seen in Figure 8, Constellations B’s phase plane in the years after the first ten are more consistent with the first ten years. In fact, the behavior in the first 10 years bounds the remaining 90 years.

The average folds of coverage as a percentage of the Moon’s surface area have been computed for 10 years with the results tabulated Table 3.

**Table 3: Average Folds of Coverage over 10 Years for Global Constellation B**

Fold of Coverage	Average % Surface Area Covered
0-fold (no coverage)	0.00004
1-fold or more	99.99996
2-folds or more	95.7
3-folds or more	45.8
4-folds	5.7

As with the prior constellation, there are a small number of short outages. For the 2 year statistics, the total duration of the gaps was 138 minutes, slightly more than with Constellation A. The details of the gaps can be seen in Figure 11. Unlike Constellation A that showed more periodic outages, this constellation has a grouping near 100 days that doesn’t appear later in the propagation. The source of this outage is still under investigation. However, as with the first constellation, this constellation provides persistent coverage for the 10 year period with the majority of the time providing 2-fold coverage.

## CONCLUSIONS

It has been found that a Polar coverage constellation of 3 satellites developed in a prior study (Ref. [1]) continues to provide 2-fold continuous coverage to a South Pole station for a 10 year period under the influence of gravitational *and* solar radiation pressure accelerations. The accommodation for solar radiation pressure was simply to re-tune the semi-major axis values to eliminate any secular drift in relative mean anomaly introduced by this acceleration. The fundamental conclusion is that this constellation provides persistent South Pole coverage without the need for any active deterministic orbit control.

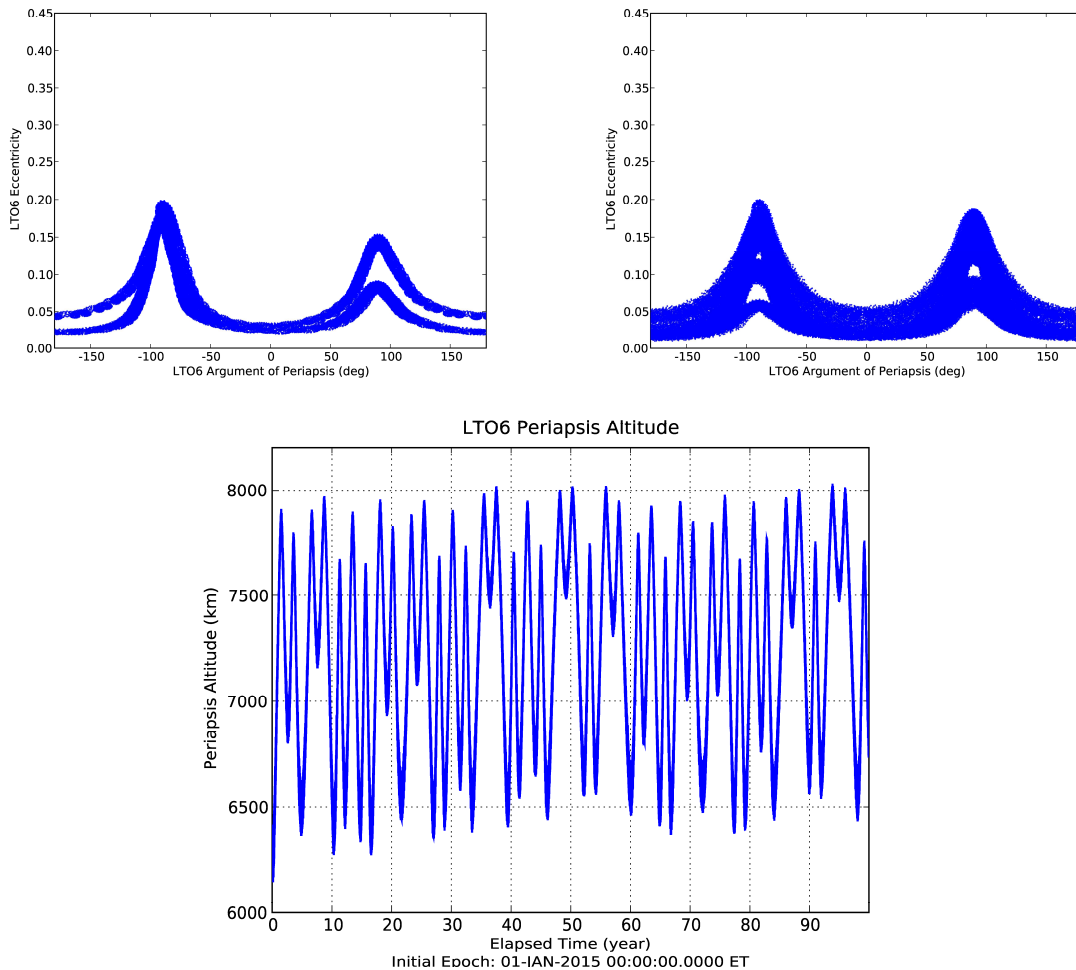


**Figure 10:** Global Constellation B's 6<sup>th</sup> satellite  $e - \omega^{\text{op}}$  phase plane for 10 years (upper left) and 100 (upper right), and periapsis altitude for the 100 years (lower).

A search for global coverage constellations utilizing a circulation in the  $e - \omega^{\text{op}}$  phase plane was conducted. Two constellations were designed using the methodology developed for the Polar coverage constellation. The constellations consisted of 6 satellites, and were found to have two planes separated by  $90^\circ$  in ascending node and apoapsis in opposite orientations between planes. Figuratively, the planes form a *linked-chain*. As with the Polar coverage constellation, these constellations are capable of providing nearly continuous global for the duration of the 10 year period under investigation without the need for any active orbit control.

Stability of the constellation's orbits is a key consideration, and specific numerical evidence suggesting bounded stability for periods up to 100 years was found. However, complex motions illustrating chaotic transitions between circulation and libration were also discovered. More conclusive statements about the nature of these complex motions can be obtained with a thorough study of the phase space using mean element propagations. This is the subject of a future study.

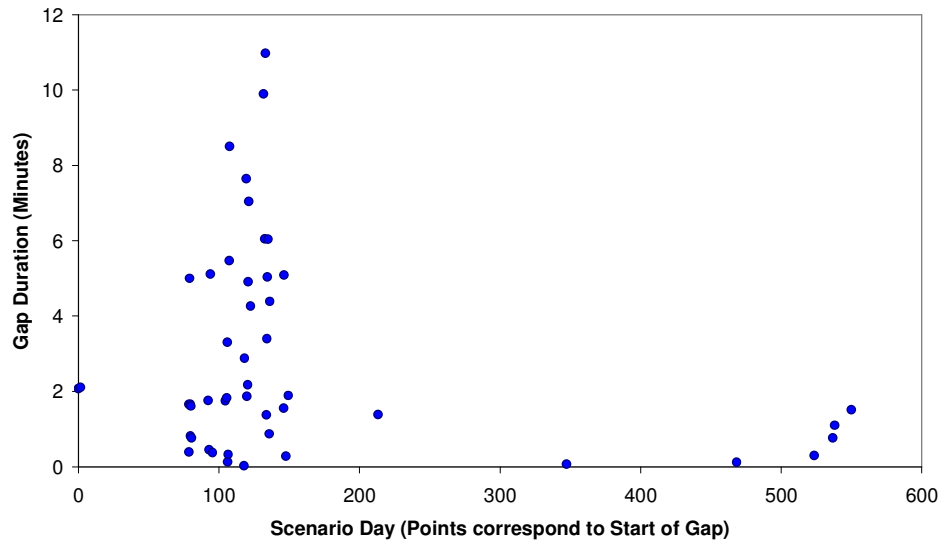


**Figure 11:** Constellation B’s coverage outage history in its first two years.

## ACKNOWLEDGEMENTS

This work was carried out in part at the Jet Propulsion Laboratory, California Institute of Technology, under contract with the National Aeronautics and Space Administration.

## REFERENCES

1. Ely, T. A., “Stable Constellations of Elliptical Inclined Lunar Orbits.” To appear in the The Journal of Astronautical Sciences.
2. Giacaglia, G., E., O., “Third Body Perturbations on Satellites”, Proceedings of the Artificial Satellite Theory Workshop, U.S. Naval Observatory, November 8-9, 1993.
3. Walker, J. G., “Continuous Whole Earth Coverage by Circular Orbit Satellites.” Proc. International Conference on Satellite Systems for Mobile Communications and Surveillance, March 1973 (Institution of Electrical Engineers, London), pp. 35 – 38.